

Shoulder Abduction in Response to Supraspinatus and Coracohumeral Ligament Tears

by

Austin Joseph Cook

Bachelor of Science in Bioengineering, University of Pittsburgh, 2021

Submitted to the Graduate Faculty of the
Swanson School of Engineering in partial fulfillment
of the requirements for the degree of
Master of Science in Mechanical Engineering

University of Pittsburgh

2023

UNIVERSITY OF PITTSBURGH
SWANSON SCHOOL OF ENGINEERING

This thesis was presented

by

Austin Joseph Cook

It was defended on

April 7, 2023

and approved by

Mark C. Miller PhD, Associate Research Professor, Mechanical Engineering and Materials
Science

Jeen-Shang Lin PhD, Associate Research Professor, Civil and Environmental Engineering

Thesis Advisor: Patrick J. Smolinski PhD, Associate Professor, Mechanical Engineering and
Materials Science

Copyright © by Austin Joseph Cook

2023

Shoulder Abduction in Response to Supraspinatus and Coracohumeral Ligament Tears

Austin Joseph Cook, B.S.

University of Pittsburgh, 2023

The rotator cuff consists of four primary muscles: the supraspinatus (SS), the infraspinatus (IS), the teres minor, and the subscapularis (SSc). In addition to these muscles, the coracohumeral ligament (CHL) supports the shoulder capsule and helps provide stability. Within the supraspinatus, there are two distinct structures: the anterior “cord” and the posterior “strap” portion. The aim of this study was threefold: to simulate tears in the cord and strap and measure shoulder abduction force, to create full tears in the cord, strap, and CHL (and once again measure shoulder abduction), and thirdly, to examine the anatomical structures more deeply using 3D scanning technology.

Physiological loading was applied to 20 cadaveric specimens using a custom shoulder simulator in order to replicate anatomical shoulder abduction in the scapular plane. Each specimen first underwent a series of loading cases, where different loads were applied to mimic four different load transmission cases. Then, each specimen underwent a cutting sequence where the first incision was randomized between the CHL or the cord. After testing in the shoulder simulator was completed and abduction force was measured, the rotator cuff muscles were removed from each shoulder at their insertion. The supraspinatus (cord and strap), infraspinatus, and CHL were then scanned with a FARO Arm 3D Scanner. Muscle and tendon cross sectional areas, thicknesses, and humeral insertion measurements were taken.

Both the modeled SS cord and SS strap tears with full force compensation were able to produce similar abduction strength to the native case, at both 0° ($p \geq 0.291$) and 30° ($p \geq 0.423$) of

abduction. Furthermore, a torn CHL did not produce significant abduction strength loss in comparison to the native state ($p>0.999$), but a torn SS cord did produce significant strength loss compared to the native ($p=0.030$).

The findings show that if the SS cord is damaged, the SS strap will compensate and will be capable of producing the same abduction strength as a native state. Additionally, an intact SS cord will compensate for a torn SS strap. This is clinically relevant, as it suggests that small anterior rotator cuff tears (<10 mm width) can be viewed as conservatively.

Table of Contents

Preface.....	xi
1.0 Introduction.....	1
1.1 Background.....	1
1.2 Motivation and Goals.....	2
1.3 Anatomy	3
1.3.1 General Anatomy	3
1.3.2 Shoulder Anatomy	6
1.4 Shoulder Machine.....	8
1.4.1 Shoulder Abduction Force	8
1.4.2 Shoulder Machine Improvements	9
2.0 Methods.....	10
2.1 Overview.....	10
2.2 Specimen Preparation	11
2.3 Testing Protocol	13
2.3.1 General Shoulder Machine Loading Procedure.....	13
2.3.2 Cord vs. Strap Loading Cases.....	14
2.3.3 Cord vs. CHL Cutting Cases.....	15
2.4 3D Scanning	16
2.5 Data Analysis and Statistics.....	19
2.5.1 A Priori Power Analysis	19
2.5.2 Statistics: Cord vs. Strap	20

2.5.3 Statistics: Cord vs. CHL	20
2.5.4 Statistics: Tendon Scanning Measurements	20
3.0 Results	22
3.1 Abduction Force: Cord vs. Strap Loading Cases	22
3.2 Abduction Force: Cord vs. CHL Cutting Cases	25
3.3 Tendon Scanning Measurements	29
4.0 Discussion and Conclusions	30
Appendix A MATLAB Code.....	33
Appendix A.1 Randomization MATLAB Code for Loading Case Sequences.....	33
Appendix A.2 Randomization MATLAB Code for Cutting Sequence.....	33
Bibliography	35

List of Tables

**Table 1. Loading cases for SS cord and SS strap comparisons. All force values in Newtons.
..... 14**

Table 2. Cutting sequences for two groups: CHL cut first and SS cord cut first. 16

**Table 3. Averages for each load case in Newtons, the percentage of the native force, and p-
values comparing each case to the native state, at both 0° and 30° 24**

**Table 4. Abduction force values for CHL-first cuts and SS Cord-first cuts, at both 0° and
30° 28**

Table 5. All measurements for 3-D scanned tendons and humeral insertions. 29

List of Figures

Figure 1. A: Intact SS muscle. B: Anterior SS cord (left) and posterior SS strap (right) heads of the SS. (https://doi.org/10.1067/mse.2000.108387).....	1
Figure 2. Human figure standing in standard anatomical position, with arms by the side, feet facing forward, and palms turned forward. (https://commons.wikimedia.org/wiki/File:Anatomical_Position.png)	4
Figure 3. Human figure with depiction of three anatomical planes: transverse, frontal, sagittal planes. (https://human-memory.net/anatomical-planes-of-body/).....	5
Figure 4. Scapular plane viewed from above, roughly 40° anterior to the frontal plane. (https://b-reddy.org/are-you-sure-youre-in-the-scapular-plane/)	6
Figure 5. The muscles of the rotator cuff from an anterior and posterior view: the supraspinatus, infraspinatus, teres minor, and subscapularis. (https://your-shoulder.com/rotator-cuff-tear-pain/).....	7
Figure 6. Custom-built shoulder machine.	8
Figure 7. Newly created shoulder machine clamp and holder for 6-DOF load cell.....	9
Figure 8. Shoulder dissected down to the muscular level. Widths for CHL, SS cord, SS strap, infraspinatus inked with surgical marker.	12
Figure 9. Tendons mounted in functional fixator for scanning.....	17
Figure 10. Humeral insertions painted and photographed.....	17
Figure 11. Tendons scanned in Geometric Software. Red dotted line shows the half-distance between the musculotendinous junction and footprint. CHL is shown in white, SS Cord in black, SS Strap in yellow, and the infraspinatus in red.	18

Figure 12. Humeral insertions outlined and labeled in Geomagic software. 19

Figure 13. Abduction force values for all loading cases. Cases with no compensating force (Cord: 0 N, Strap: 24 N and Cord: 56 N, Strap: 0 N) are designated by the striped bars, and full load compensation cases (Cord: 0 N, Strap: 80 N and Cord: 80 N, Strap: 0 N) 23

Figure 14. Abduction force values for the CHL-first group, with the successive cuts going from left to right..... 26

Figure 15. Abduction force values for the SS Cord-first group, with successive cuts going from left to right..... 27

Preface

I would like to thank both Dr. Mark Miller and Dr. Patrick Smolinski for their guidance in engineering principles and developing my research skills further. Their knowledge and expertise in the field has been invaluable. I also wish to thank Dr. Christopher Schmidt for his generosity, leadership, and continued encouragement to strive for excellence. Additional thanks go to others who have supported me through this endeavor, including Justin Buce, Sean Cooke, Dr. Joshua Dworkin, and Dr. Omar Rodriguez.

1.0 Introduction

1.1 Background

The supraspinatus (SS) muscle is one of the four main rotator cuff muscles. Its primary functions are to assist in shoulder abduction and to stabilize the glenohumeral joint¹. The SS can be split into its two muscular heads, the anterior bipennate “cord” named for the thicker cord-like appearance of the anterior portion and posterior unipennate “strap,” the thinner posterior head. The SS cord has a larger physiologic cross-sectional area of 140 mm² and a length of 5.4 cm², while the SS strap has a smaller cross-sectional area of 62 mm² and length of 2.8 cm³ (Figure 1).

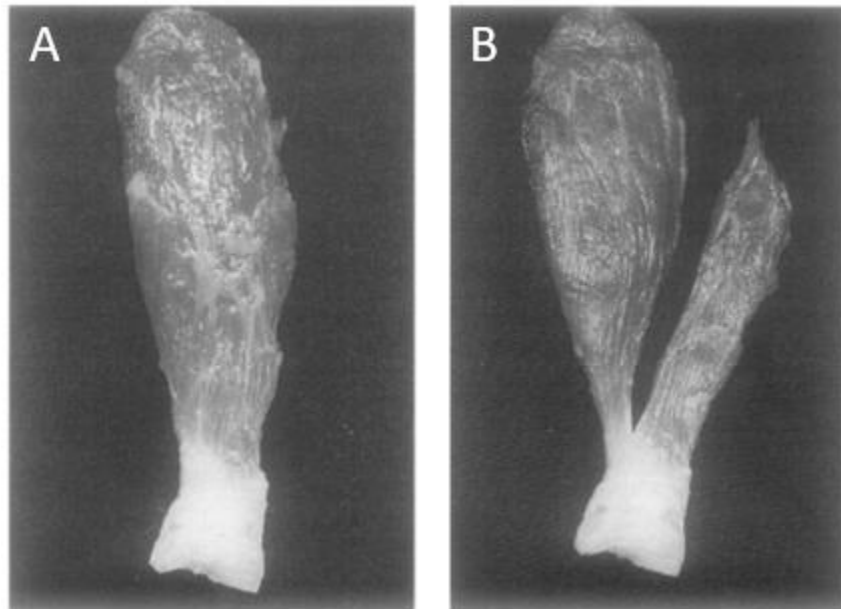


Figure 1. A: Intact SS muscle. B: Anterior SS cord (left) and posterior SS strap (right) heads of the SS.

(<https://doi.org/10.1067/mse.2000.108387>.)

While the anatomy of the two SS heads has been thoroughly examined, the mechanical individual contributions from the SS cord and SS strap to shoulder abduction strength have not been studied extensively.

Another important structure within the rotator cuff complex is the coracohumeral ligament (CHL). The CHL is a ligament, not a muscle, and is believed to strengthen the shoulder joint capsule⁴. The contribution of the CHL in shoulder abduction has not been thoroughly studied; it may only contribute to stability, or it may also assist in force transmission, particularly with the SS cord immediately adjacent to it.

1.2 Motivation and Goals

Rotator cuff tears are highly prevalent among adults and have significant impacts on shoulder abduction strength. Among rotator cuff tears, the majority occur within the supraspinatus muscle⁵. Due to this common disruption of the supraspinatus and shoulder function, the goal of this study is to examine the effects of simulated and real tears of the SS cord, SS strap, and CHL and document the related anatomy of these structures.

Exploration of the relationship between supraspinatus tears and abduction force can help to inform surgical intervention. Significant loss in strength leads to patients seeking medical attention⁶ and finding a sharp decrease in strength due to supraspinatus deficiencies could provide surgeons with a benchmark identifier as to when surgical intervention is important. If the SS cord or SS strap is determined to be less important in abduction strength, this may allow for different surgical approaches when tears are identified. If, perhaps, the CHL is found to be important in shoulder abduction strength, this might also change surgeons' approach to CHL tears.

This study closely examines function and anatomy of three structures (SS cord, SS strap, and CHL) and thus there are multiple hypotheses for the outcomes of this examination. 1) For the modeled SS cord and SS strap tears, we hypothesize that a shoulder with a torn SS cord (no force compensation) will be able to generate less force than a shoulder with a SS strap tear (no force compensation), and that an intact SS cord will be able to offset a torn SS strap with full force compensation, but not the other way around. 2) For the SS cord and CHL tears, we hypothesize that a torn CHL will not result in a significant loss of abduction strength, but a torn SS cord will produce a significant loss of strength. This outcome is hypothesized to hold true regardless of the order of the SS cord and CHL tears. 3) When looking at the tendon anatomy, we hypothesize that the SS cord will be thicker mediolaterally than the SS strap and the SS Strap will have a larger area than the SS cord.

1.3 Anatomy

1.3.1 General Anatomy

A universal language for describing the human body is used in medicine to readily identify planes of motion and anatomical structures relative to each other. That language will be used in the following sections and is outlined here. The body is typically viewed in the standard anatomical position, shown in Figure 2, with the toes and palms of the hands facing forward.

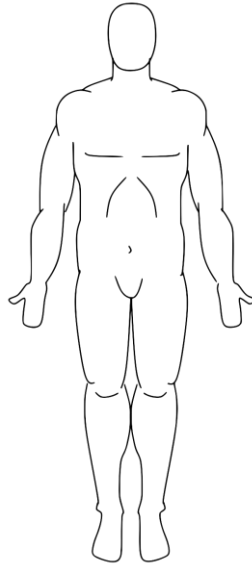


Figure 2. Human figure standing in standard anatomical position, with arms by the side, feet facing forward, and palms turned forward. (https://commons.wikimedia.org/wiki/File:Anatomical_Position.png)

In this configuration, the *anterior* direction is used to describe the front of the body, or forward, and *posterior* backward. Structures closer to the middle of the body are described as *medial*, and body parts further from the center are relatively *lateral*. *Superior* refers to anatomical structures closer to the head, and *inferior* refers to those lower, closer to the ground.

There are three anatomical planes that divide the entire body into regions and assist in describing motion, as well as one plane specific to the shoulder. The transverse plane divides the body into top and bottom halves, and can be used to describe anterior, posterior, medial, or lateral translation. The frontal plane splits the body into front and back portions and describes superior, inferior, medial, and lateral movement. Thirdly, the sagittal plane contains anterior, posterior, superior, and inferior movement by splitting the body into right and left halves. These planes are shown in Figure 3 with the body in standard anatomical position.

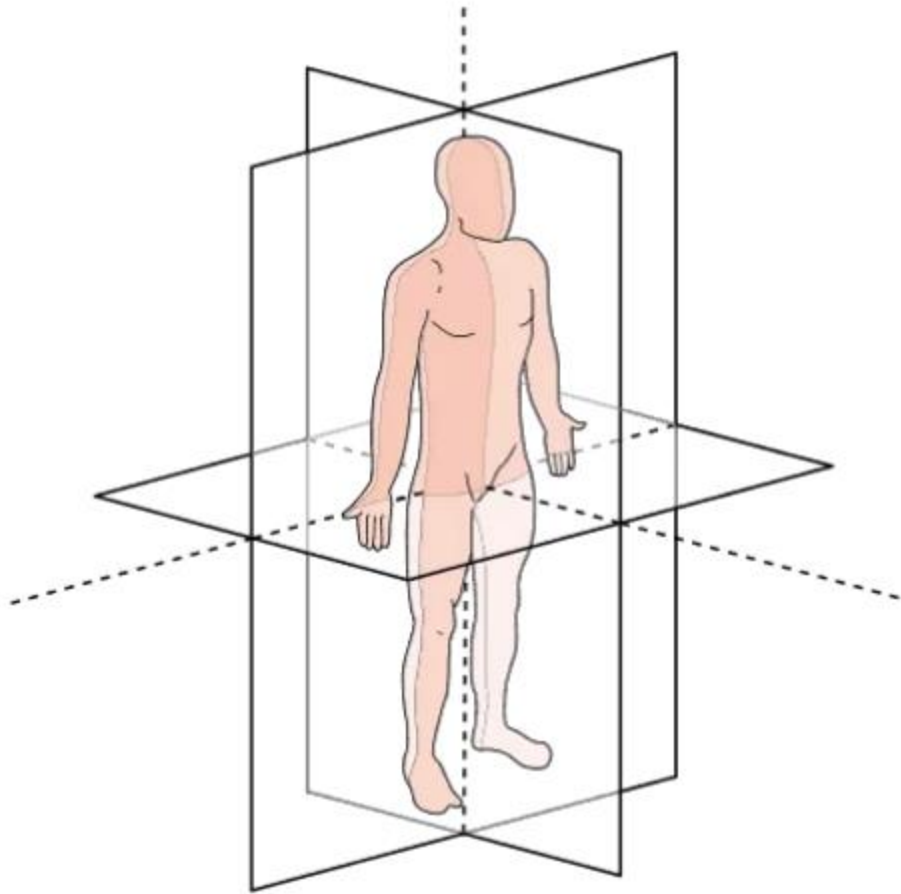


Figure 3. Human figure with depiction of three anatomical planes: transverse, frontal, sagittal planes.

(<https://human-memory.net/anatomical-planes-of-body/>)

Additionally, the scapular plane is helpful in describing shoulder motion. The scapula is positioned at an angle and is roughly 40° anterior to the frontal plane⁷. Shown in Figure 4, the scapular plane contains the optimal path of motion for shoulder abduction⁸.

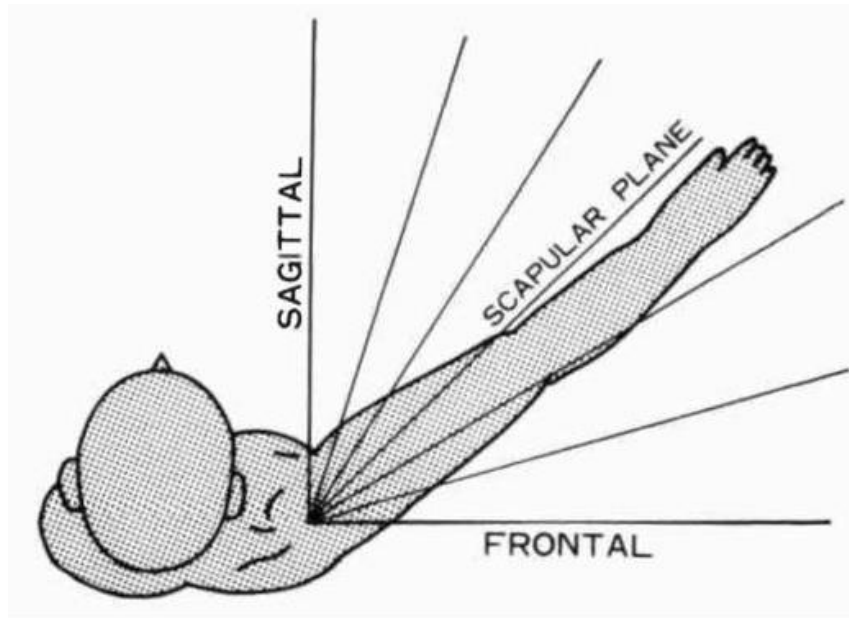


Figure 4. Scapular plane viewed from above, roughly 40° anterior to the frontal plane. (<https://b-reddy.org/are-you-sure-youre-in-the-scapular-plane/>)

1.3.2 Shoulder Anatomy

The shoulder is a complex anatomical formation, consisting of three bones and many muscles and ligaments. The scapula articulates with the head of the humerus to form a ball-and-socket joint, allowing for movement in all directions. This connection is called the glenohumeral joint, named for the points of contact between the scapula's glenoid, and the humerus. The clavicle works alongside the scapula to form the pectoral girdle, allowing for increased range of motion in the shoulder, while assisting the scapula in force transmission.

The primary muscles that act through this wide range of motion are the rotator cuff muscles: the supraspinatus, infraspinatus, teres minor, and subscapularis (Figure 5). The rotator cuff muscles provide important stabilization to the shoulder unit as a whole and also serve to abduct and rotate the arm. Specifically, the supraspinatus is the primary agent among the four rotator cuff

muscles that abducts the arm, while the infraspinatus, teres minor, and subscapularis function in rotation and stabilization⁹.

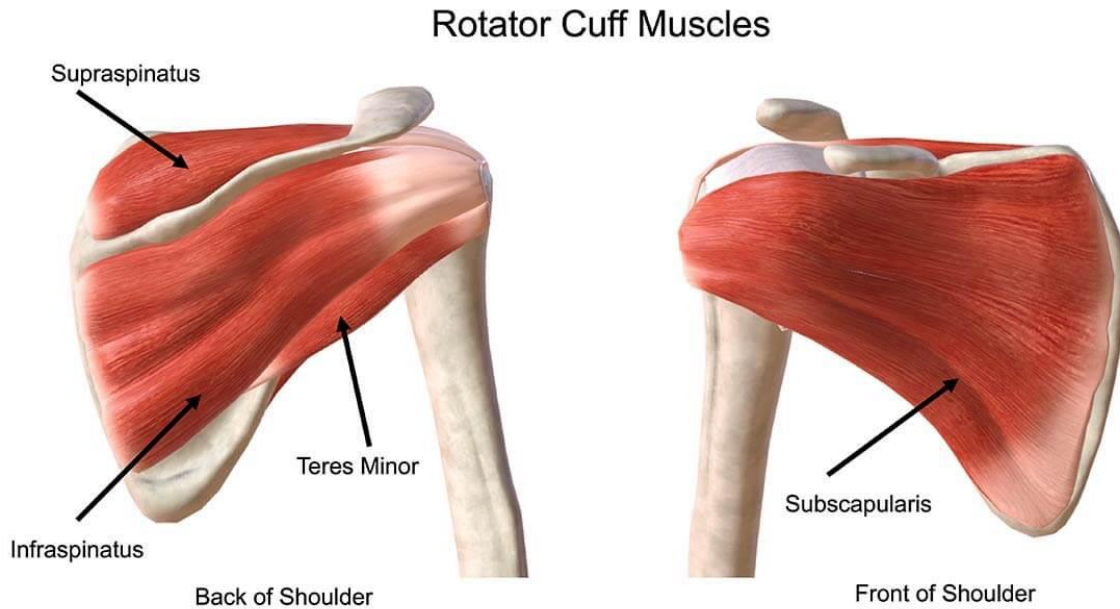


Figure 5. The muscles of the rotator cuff from an anterior and posterior view: the supraspinatus, infraspinatus, teres minor, and subscapularis. (<https://your-shoulder.com/rotator-cuff-tear-pain/>)

The supraspinatus can be split into two muscular units, the anterior portion and the posterior portion. The anterior head (“SS cord”) has a larger cross-sectional area than the posterior head¹ (“SS strap”) and is shown previously in Figure 1.

The CHL is also a focus in this study. It has been described as originating from the coracoid process and inserting into the greater and lesser tubercles¹⁰. The CHL rests above the subscapularis¹¹; it provides structural support and increased range of motion to the glenohumeral joint¹². The CHL’s role in force transmission regarding shoulder abduction is poorly documented, and this project looks to examine this role.

1.4 Shoulder Machine

1.4.1 Shoulder Abduction Force

A custom-built shoulder abduction machine was constructed to apply specific loads to distinct muscles and simulate shoulder abduction (Figure 6). Consisting of six servo actuators (Parker Hannifin Corp., Cleveland, OH), six single-DOF load cells ((MLP-100, Transducer Techniques, Inc., Temecula, CA) (Accuracy $\pm 0.25\%$ RO, Nonrepeatability $\pm 0.05\%$ RO), and two 6-DOF load cells (Bertec Corp., Columbus, OH), forces could be applied to muscles at both 0° and 30° of abduction.

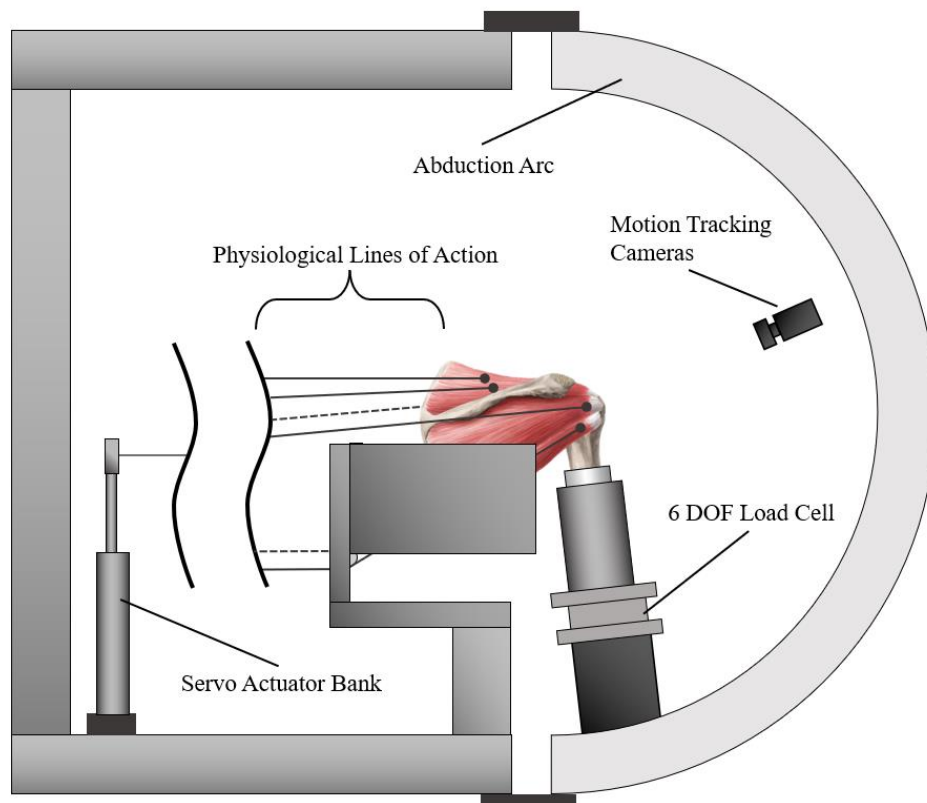


Figure 6. Custom-built shoulder machine.

1.4.2 Shoulder Machine Improvements

For the needs of this experiment, an additional load cell was required for the shoulder simulator. Originally, there was a single 6-DOF load cell at the distal humerus and no load cell on the scapular side of the glenohumeral joint. For the purposes of this study, a scapular mount was manufactured and implemented so that a second 6-DOF load cell would measure forces on the scapular side of the glenohumeral joint. This required creating a base attached to the metal framework of the shoulder machine that would house the second 6-DOF load cell and a clamp to stabilize the glenoid (Figure 7). This process was completed in the University of Pittsburgh Swanson Center for Product Innovation.

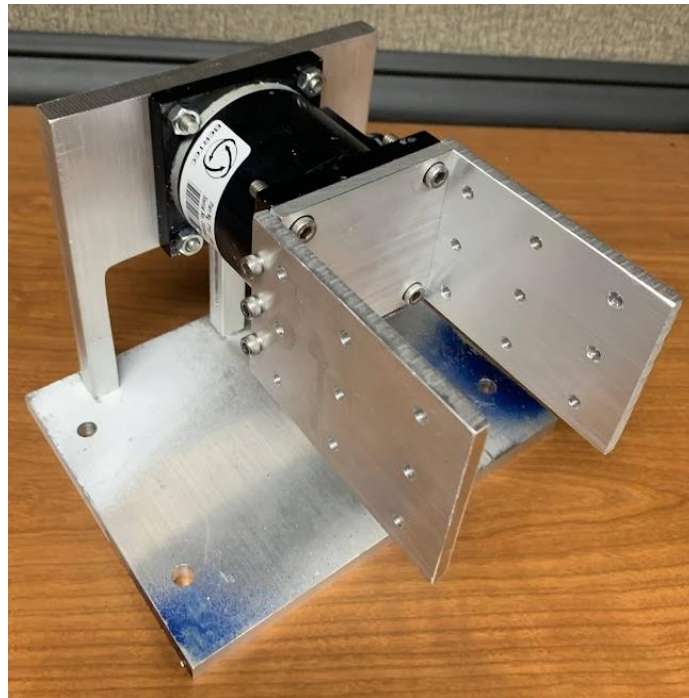


Figure 7. Newly created shoulder machine clamp and holder for 6-DOF load cell.

2.0 Methods

2.1 Overview

Twenty fresh-frozen cadaveric shoulders (69.10 ± 10.64 years) were loaded with physiological forces applied to five rotator cuff muscles to simulate shoulder abduction. A native case and four distinct loading cases were randomized and applied (Appendix A.1) to the muscles to model SS tears and examine differences in abduction force recovery for the SS cord and SS strap. The loading cases were all compared to determine whether the SS cord or SS strap was able to fully recover abduction force when the other head was unloaded. After this, a randomized cutting sequence (Appendix A.2) was implemented, starting with cutting either the SS cord or the CHL, then the other, followed by cutting the SS strap and then infraspinatus. Shoulder abduction force was measured at the distal humerus and additional forces measured at the medial scapular border. The two groups (either the cord was cut first, or the CHL was cut first) were compared to determine differences in abduction force without the cord or without the CHL.

After all loading and cutting cases were complete, the muscles were dissected from the humerus and mounted to a functional fixator. The CHL, SS cord, SS strap, and infraspinatus were all scanned using a laser scanning system (FaroArm, FL, USA) and Geomagic Software (3D Systems, NC, USA). Within the 3D software, the muscles and CHL were measured at the half-distance between the medial footprint border and the musculotendinous junction. A cross-sectional slice was taken at this location and the borders were outlined. The areas and mediolateral thicknesses were computed.

2.2 Specimen Preparation

Forty-five fresh-frozen cadavers were obtained for this study and exclusion criteria of glenohumeral arthritis or rotator cuff pathology was established. Twenty specimens (69.10 ± 10.64 years) were identified as viable for this study. Soft tissue down to the muscular level was excised from each specimen, and the humerus was transected at its midpoint. An acromionectomy was performed and all extraneous soft tissue was removed from the muscles and bones to reveal the supraspinatus, infraspinatus, teres minor, subscapularis, and CHL. Braided #2 sutures were lock stitched and threaded into these muscle bellies immediately medial to the musculotendinous junction; special care was taken to split the two heads of the supraspinatus with sutures in each head. Six sutures were needed in total: SS cord, SS strap, infraspinatus, teres minor, upper subscapularis, and lower subscapularis. All sutures were tied to 80 lb. proof fishing line connected to the shoulder machine's actuators. Anteroposterior widths of the CHL, SS cord, SS strap, and infraspinatus at the medial footprint were measured with a scientific caliper (accuracy 0.001 mm) and marked out with a surgical marker (Figure 8).

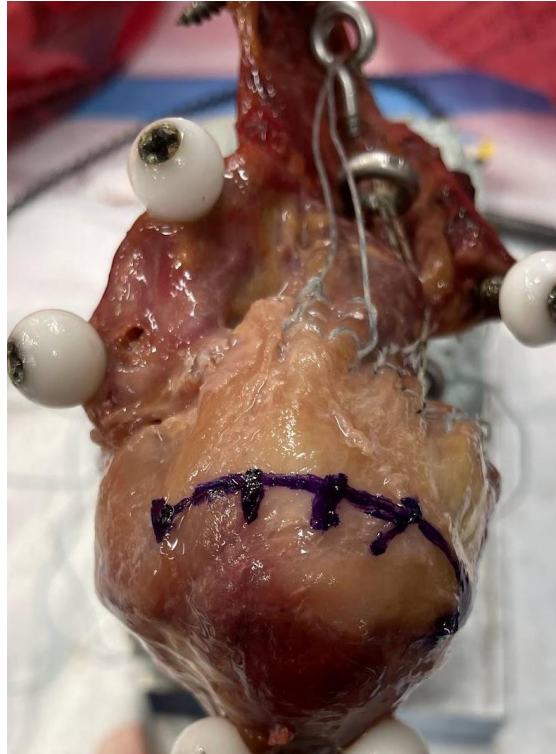


Figure 8. Shoulder dissected down to the muscular level. Widths for CHL, SS cord, SS strap, infraspinatus inked with surgical marker.

The portions of each muscle medial to the musculotendinous junction and suture attachment were removed. Eyelet screws were threaded into the supraspinatus fossa, infraspinatus fossa, subscapular fossa, and the medial border of the scapula. These eyelets served to guide the sutures along the muscular lines of action for abduction. The scapula was placed inside a custom, metal box and surrounded by hardening resin (Bondo, 3M). A Kirschner wire was drilled into the humeral head and used to ensure that the scapular and humeral complex was aligned correctly in the box. This wire was later removed. Plastic tubing was used to create paths through the resin for the lower subscapularis and teres minor lines of pull. When the resin hardened, the scapula was held firmly in a rectangular mold that would later be secured in the holding mechanism of the shoulder machine. The distal humerus followed a similar procedure; it was placed in a PVC sleeve

with the same hardening resin that allowed the PVC to be inserted into the metal cylinder of the humeral arm portion of the shoulder machine. A line was drawn down the center of the PVC sleeve to highlight internal or external rotation.

The hardening resin holding the scapula was screwed into the holding mechanism of the shoulder machine using three wood screws. These three points of contact kept the scapula from rotating. The sutures were attached to individual actuators of the shoulder machine with 80 lb. proof fishing line, so that unique loads could be applied to each muscle. The PVC sleeve housing the humerus was fitted into the distal arm within the abduction arc. The sleeve was allowed to freely internally or externally rotate and to move axially up and down within the metal cylinder. The most distal part of the arm was locked into place within the abduction arc, using two metal clamps. The rationale of restricting abduction motion was to enable the distal 6-DOF load cell to measure abduction strength.

2.3 Testing Protocol

2.3.1 General Shoulder Machine Loading Procedure

The humeral head was centered in the glenoid by a trained orthopaedic fellow. The correct positioning was verified by a C-arm X-ray machine. Then the sutures were each loaded to 10N of force to hold the humeral head tightly to the glenoid. Two distinct testing procedures were followed, loading cases and cutting cases, detailed in the following sections. For both procedures, the same shoulder simulator conditions were applied, and data was gathered at 50 Hz. The simulator loaded the actuators from 10 N to the desired values and then systematically varied

between the desired value and half of the desired value to eliminate hysteresis. Each load was applied until it had peaked four times, and the fourth peak was averaged over 0.1 seconds for the resulting abduction strength. The force perpendicular to the humeral arm was taken from the distal humerus 6-DOF load cell as the abduction force.

2.3.2 Cord vs. Strap Loading Cases

The first testing sequence examined shoulder abduction strength of the SS cord and SS strap. Tears were modeled by applying different loading cases to each head of the supraspinatus. The different cases were randomized using a MATLAB code (Appendix A.1) and are shown below in Table 1. The physiological loads came from previously published literature focusing on the cross-sectional area of muscles and the corresponding electromyographic activity^{13,14}.

Table 1. Loading cases for SS cord and SS strap comparisons. All force values in Newtons.

Case	SS Cord [N]	SS Strap [N]	Infraspinatus [N]	Upper Subscap. [N]	Lower Subscap. [N]	Teres Minor [N]
Native	56	24	90	127	108	97
Case 1	0	24	90	127	108	97
Case 2	0	80	90	127	108	97
Case 3	56	0	90	127	108	97
Case 4	80	0	90	127	108	97

The first case shown in Table 1 was designated as the “Native” case, where all muscles underwent the forces they normally would with no aberration in the rotator cuff. The loads applied to the infraspinatus, upper and lower subscapularis, and teres minor remained constant throughout all five conditions. However, the SS cord and SS strap had different force values for each case. These numbers came from the cross-sectional area of the muscle bellies¹. Using the aforementioned cross-sectional areas of 140 mm² and 62 mm² for the SS cord and SS strap, respectively, the loads were proportioned to recreate different force transmission scenarios seen in Table 1.

The various load cases replicated different potential loading patterns of individuals with supraspinatus tears. The SS cord was loaded with 0, 56, or 80N, while the SS strap was loaded with 0, 24, or 80N. Case 1 modeled a SS cord tear with no force through the SS strap, Case 2 modeled the same tear with full load compensation (or load transfer) from the torn SS cord to the SS strap. Case 3 modeled a torn SS strap with no load through the SS cord, and Case 4 modeled a SS strap tear with full load compensation to the SS cord. All cases were completed at 0° and 30° of humeral abduction and were replicated twice. All force values were recorded during the fourth loading peak.

2.3.3 Cord vs. CHL Cutting Cases

After the loading cases were completed, a sequence of cuts was then tested. The specimens were randomized (Appendix A.2) into one of two groups: CHL cut first or SS cord cut first. The sequences of cuts are summarized in Table 2. The forces applied to each muscle were the same as the “Native” case designated earlier and held constant for each cutting case^{13,14}.

Table 2. Cutting sequences for two groups: CHL cut first and SS cord cut first.

Group:	Cut 1	Cut 2	Cut 3	Cut 4
CHL-First	CHL	SS Cord	SS Strap	Infraspinatus
Cord-First	SS Cord	CHL	SS Strap	Infraspinatus

Each cut was performed at the humeral insertion by a trained orthopaedic fellow, using the previously determined anteroposterior widths of each structure. The muscles and CHL were all cut down to the bone, so as to release the structure entirely. The resulting visible insertion area was finely painted for the humeral insertion measurements later. Each successive cut resulted in a larger exposed area. All cases were completed at 0° and 30° of humeral abduction and were replicated twice and all force values were recorded during the fourth loading peak.

2.4 3D Scanning

After both the loading and cutting cases were completed, the specimen was removed from the machine, and the muscles were transected from the humeral head. The rotator cuff muscles were mounted on a functional fixator with the sutures used as attachment points (Figure 9). A laser scanning system (FaroArm, FL, USA) and Geomagic Software (3D Systems, NC, USA), was used to create 3D models of the CHL, SS cord, SS strap, and infraspinatus. After this, the humeral head was also scanned using the same software (Figure 10).

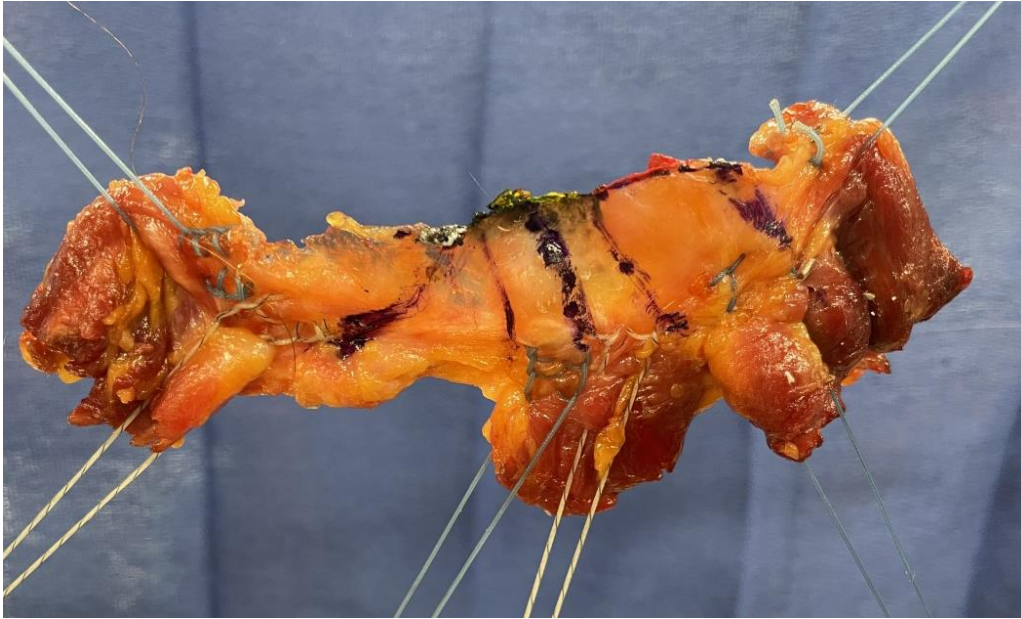


Figure 9. Tendons mounted in functional fixator for scanning.



Figure 10. Humeral insertions painted and photographed.

Within the Geomagic Software, the muscles and CHL were processed; the cross-sectional areas and mediolateral thicknesses were calculated at the half-distance between the musculotendinous junction and corresponding footprint (Figure 11). Additionally, the average of the SS cord and SS strap was used as the tendon thickness and mediolateral length for the supraspinatus at large. The humeral head was used to find insertion area, anteroposterior, and mediolateral measurements for the CHL, SS cord, SS strap, and infraspinatus insertions. The insertion of the supraspinatus as a whole was also examined, using the sum of the SS cord and SS strap measurements (Figure 12).

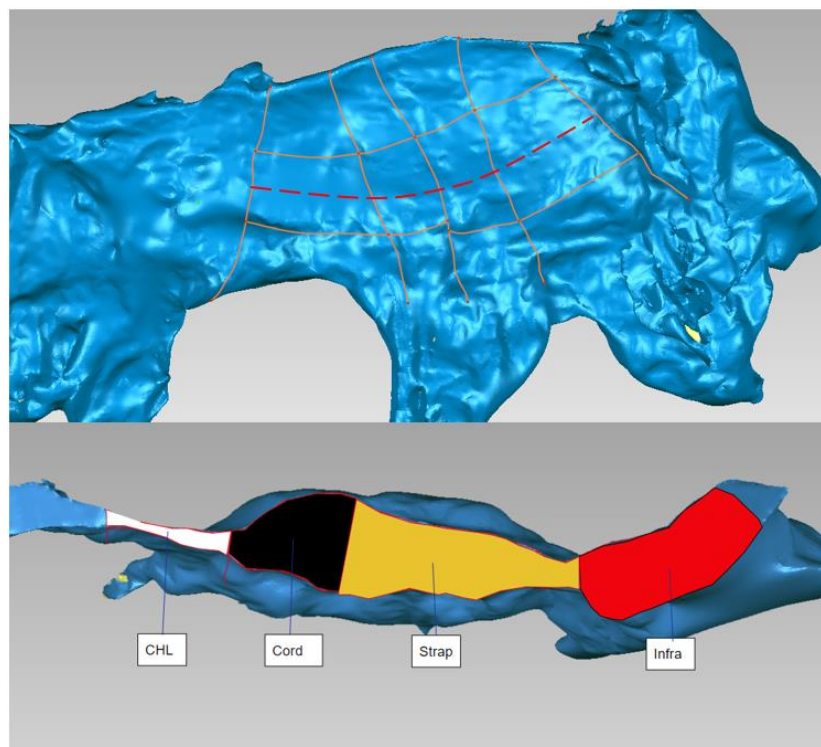


Figure 11. Tendons scanned in Geometric Software. Red dotted line shows the half-distance between the musculotendinous junction and footprint. CHL is shown in white, SS Cord in black, SS Strap in yellow, and the infraspinatus in red.

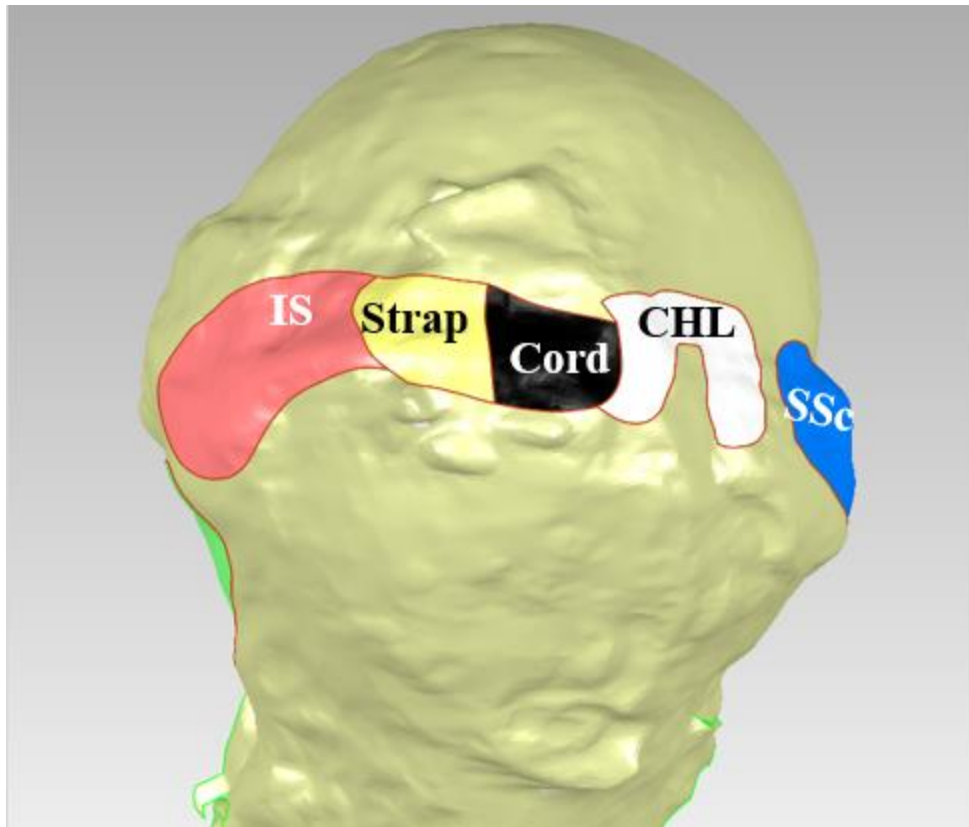


Figure 12. Humeral insertions outlined and labeled in Geomagic software.

2.5 Data Analysis and Statistics

2.5.1 A Priori Power Analysis

Previous research used to inform this study came from Rybalko et al.'s examination of partial and complete supraspinatus tears¹⁵. Their research found a drop in abduction force from 3.3 N in a partially torn supraspinatus to 1.6 N when the supraspinatus was fully torn. Based on this 52% drop in abduction force, the statistical package G*Power (G*Power, University of Düsseldorf,

Düsseldorf, Germany) was used to determine that a sample size of 20 specimens was appropriate to achieve a statistical power of 0.8 with $p=0.05$.

2.5.2 Statistics: Cord vs. Strap

In order to compare the effect of a modeled tear in the SS cord and SS strap, one two-factor repeated measures ANOVA with subsequent post hoc Bonferroni corrections (SPSS, IBM, $p<0.05$) was performed. The two factors were abduction angle and loading case. A Kolmogorov-Smirnov test was used to verify normality of data.

2.5.3 Statistics: Cord vs. CHL

Two analyses were necessary for the SS cord and CHL comparison. First, a two-factor ANOVA was used to compare the different initial cuts (SS cord or CHL), with abduction angle and cut case as the two factors. Secondly, the SS strap and infraspinatus cut were compared to the native case using a two-factor repeated measures ANOVA, with abduction angle and cut case as the factors. In this analysis, all 20 specimens were grouped together, and Bonferroni post-hoc pairwise comparisons were implemented.

2.5.4 Statistics: Tendon Scanning Measurements

Individual paired t-tests for thickness and area were performed on the SS cord and SS strap, and three ANOVAs were used for the humeral insertion areas, insertion anteroposterior widths, and insertion mediolateral lengths. Each ANOVA looked at the measurements for the CHL, SS

cord, SS strap, supraspinatus, and infraspinatus. Post-hoc t-tests with Bonferroni correction were implemented when statistical significance was found within the ANOVA.

3.0 Results

3.1 Abduction Force: Cord vs. Strap Loading Cases

The abduction force strength values are shown in Figure 13 for 0° and 30°, and the averages with p-values for each case are detailed in Table 3. The two-factor repeated measures ANOVA for SS cord and SS strap tears revealed that the abduction force was dependent on load case ($p \leq 0.001$) and dependent on abduction angle ($p = 0.010$). At 0°, the modeled SS strap tear (Case 3) produced a 27% drop in abduction force, while the modeled SS cord tear (Case 1) showed a 53% drop in abduction force. The same relationship held at 30°, with the model SS strap tear producing a 23% drop and the model SS cord tear producing a 38% drop in force. This relationship of the SS cord tear producing a greater loss in force than the SS strap tear was statistically significant at 0° ($p \leq 0.001$). Both modeled SS cord and SS strap tears without force compensation were statistically significant when compared to the native, at both 0° and 30° of abduction ($p \leq 0.001$).

The modeled SS cord and SS strap tears with full force compensation (or transfer) to the other respective head showed similar values to the native force. At both 0° and 30°, the model SS cord tear with full force transfer to the SS strap, recovered enough force that it was not significantly different from the native case ($p \geq 0.291$). Similarly, the model SS strap tear with full force compensation was not statistically different from the native case ($p \geq 0.410$), for both 0° and 30°. Between the SS cord and SS strap model tears with full force transfer, there was no significant difference ($p > 0.999$) at either 0° or 30°.

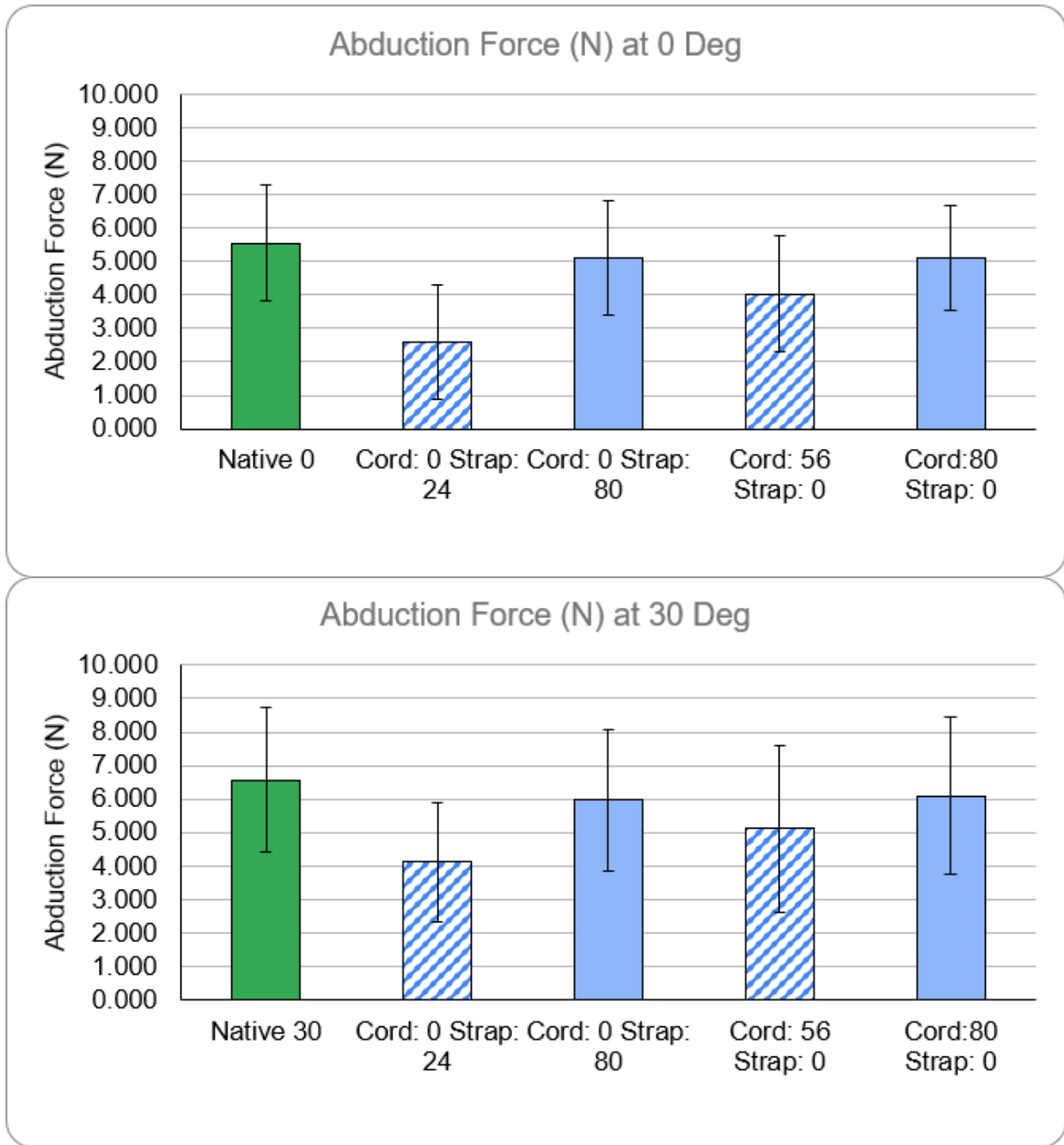


Figure 13. Abduction force values for all loading cases. Cases with no compensating force (Cord: 0 N, Strap: 24 N and Cord: 56 N, Strap: 0 N) are designated by the striped bars, and full load compensation cases (Cord: 0 N, Strap: 80 N and Cord: 80 N, Strap: 0 N)

Table 3. Averages for each load case in Newtons, the percentage of the native force, and p-values comparing each case to the native state, at both 0° and 30°

Abduction Angle	Load Case	Abduction Force [N]	Percentage of Native Force	p-value vs Native
0°	Native: Cord 56 N, Strap 24 N	5.5 (1.7)	N/A	N/A
0°	Case 1: Cord 0 N, Strap 24 N	2.6 (1.7)	47%	p<0.001
0°	Case 2: Cord 0 N, Strap 80 N	5.1 (1.7)	93%	p=0.291
0°	Case 3: Cord 56 N, Strap 0 N	4.0 (1.7)	73%	p<0.001
0°	Case 4: Cord 80 N, Strap 0 N	5.1 (1.6)	93%	p=0.410
30°	Native: Cord 56 N, Strap 0 N	6.6 (2.2)	N/A	N/A
30°	Case 1: Cord 0 N, Strap 24 N	4.1 (1.8)	62%	p<0.001
30°	Case 2: Cord 0 N, Strap 80 N	6.0 (2.1)	91%	p=0.479
30°	Case 3: Cord 56 N, Strap 0 N	5.1 (2.5)	77%	p<0.001
30°	Case 4: Cord 80 N, Strap 0 N	6.1 (2.3)	92%	p=0.423

3.2 Abduction Force: Cord vs. CHL Cutting Cases

The abduction force values for the CHL-first and SS cord-first cuts are shown in Figure 14 and Figure 15. The averages are listed in Table 4. The two-factor ANOVA looking at the first cuts showed significance for the cut case, but not for the abduction angle ($p=0.016$ and $p=0.192$, respectively). The CHL-first group showed a 3.5% drop in force when the CHL was cut at 0° and a 7.2% drop in force at 30° . When the SS cord was cut first, there was a 9.8% and 22.2% drop in abduction force for 0° and 30° , respectively. Post-hoc pairwise comparisons based on the cut case significance show that when the CHL was cut, the force was not significant compared to the native case ($p>0.999$), but when the SS cord was cut, it was significant compared to the native state ($p=0.030$).

The second two-way ANOVA that examined the SS strap and infraspinatus cuts showed significance for cut case ($p<0.001$) but not for abduction angle ($p=0.445$). Both the SS strap cut and infraspinatus cut were significant when compared to the native at 0° ($p<0.001$, $p<0.001$) and at 30° ($p=0.028$, $p<0.001$).

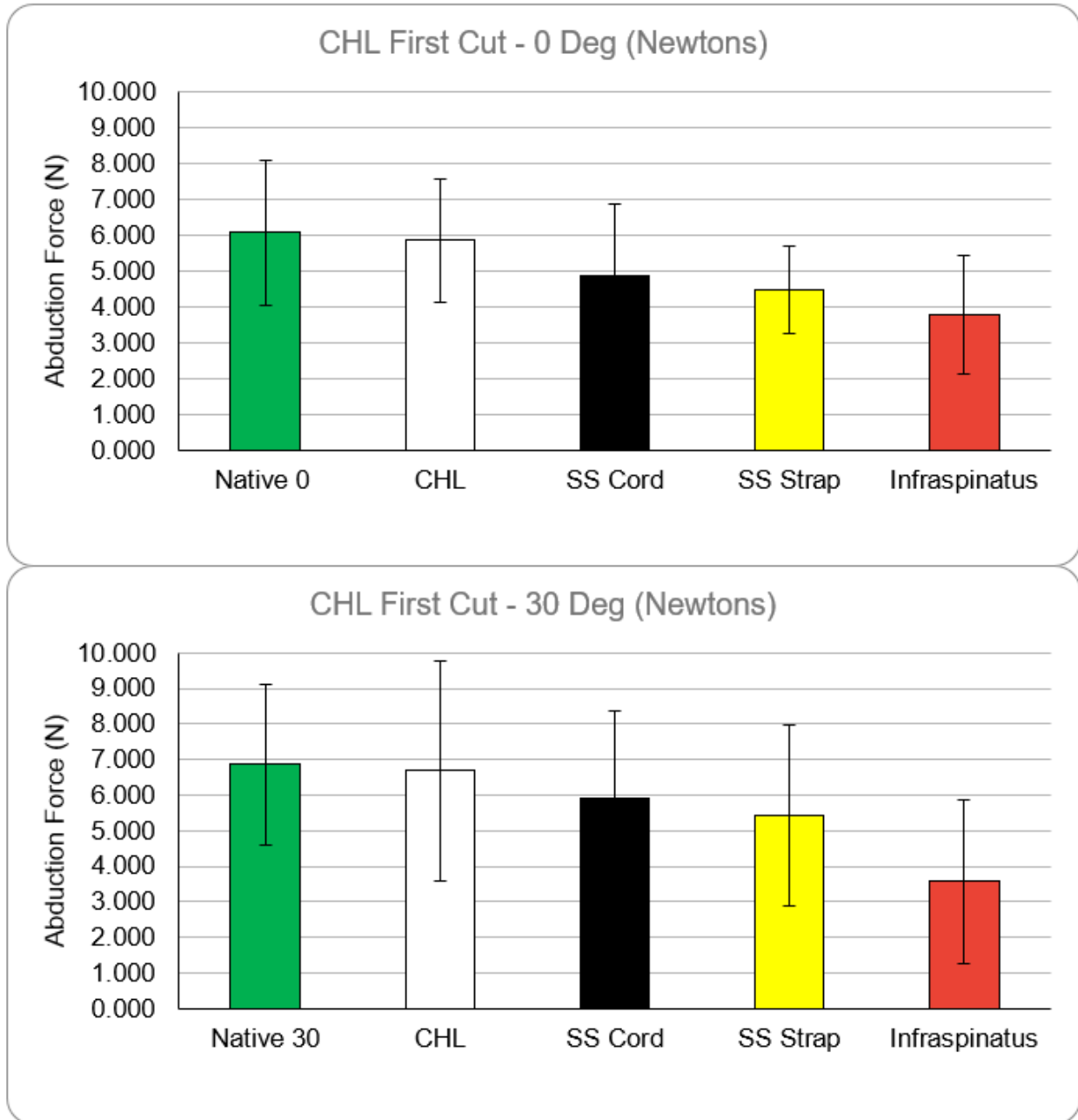


Figure 14. Abduction force values for the CHL-first group, with the successive cuts going from left to right.

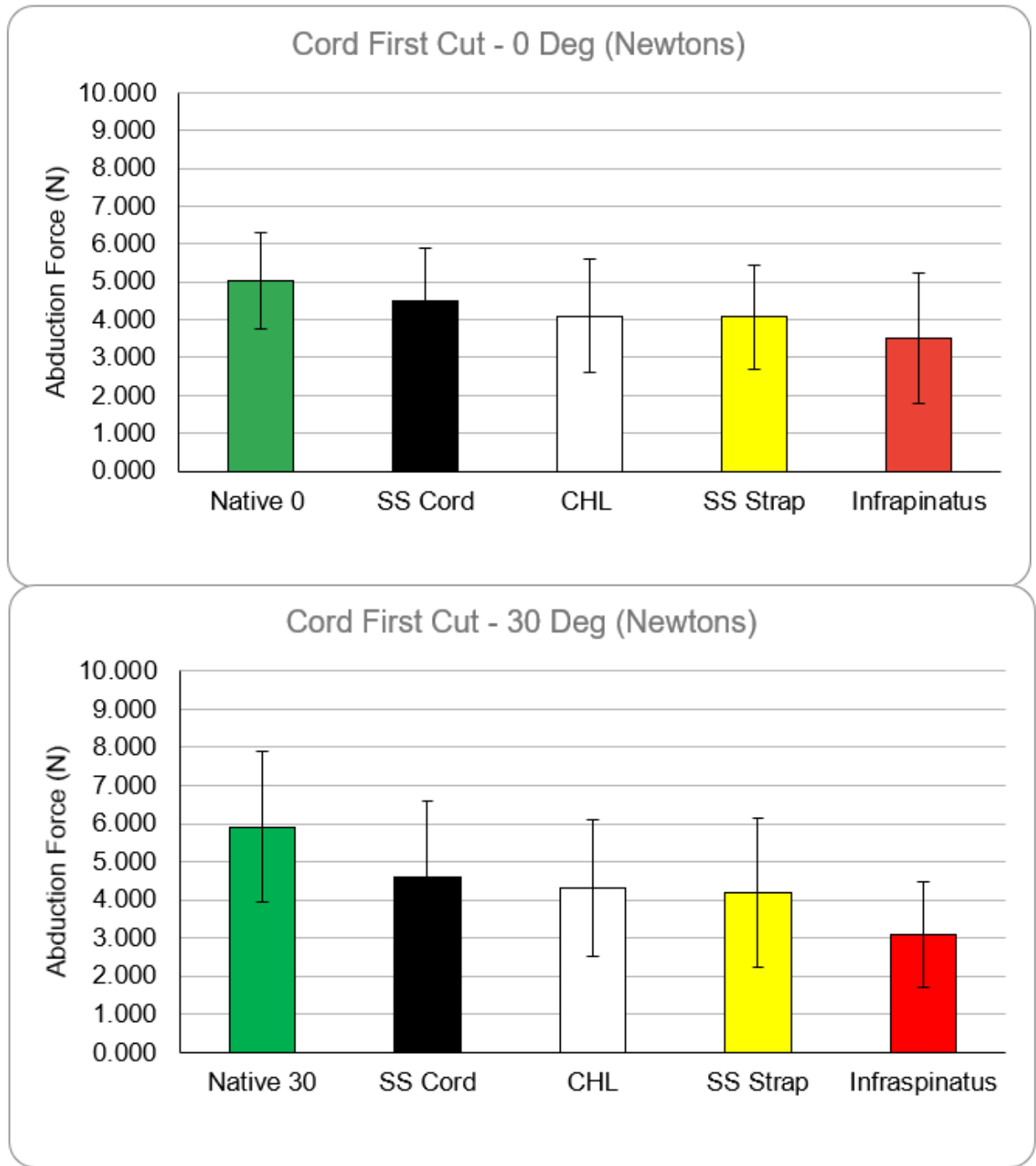


Figure 15. Abduction force values for the SS Cord-first group, with successive cuts going from left to right.

Table 4. Abduction force values for CHL-first cuts and SS Cord-first cuts, at both 0° and 30°.

Abduction Angle	Cut Structure	Abduction Force [N]
CHL-First Cut		
0°	-----	6.1 (2.0)
0°	CHL	5.9 (1.7)
0°	SS Cord	4.8 (2.0)
0°	SS Strap	4.5 (1.2)
0°	Infraspinatus	3.8 (1.7)
30°	-----	6.9 (2.2)
30°	CHL	6.7 (3.0)
30°	SS Cord	5.9 (2.5)
30°	SS Strap	5.4 (2.5)
30°	Infraspinatus	3.6 (2.3)
SS Cord-First Cut		
0°	-----	5.0 (1.3)
0°	SS Cord	4.5 (1.4)
0°	CHL	4.1 (1.5)
0°	SS Strap	4.1 (1.4)
0°	Infraspinatus	3.5 (1.7)
30°	-----	5.9 (2.0)
30°	SS Cord	4.6 (2.0)
30°	CHL	4.3 (1.8)
30°	SS Strap	4.2 (2.0)
30°	Infraspinatus	3.1 (1.4)

3.3 Tendon Scanning Measurements

All tendon and insertional area measurements are listed below in Table 5. The paired t-test looking at the tendon thickness found significance between the SS cord and SS strap ($p=0.005$), with the SS cord having a greater thickness. There was no significance among tendon areas ($p=0.159$) for the SS cord and SS strap.

Looking at the humeral insertion measurements, the SS strap had a significantly larger humeral insertion area and greater anteroposterior width than the SS cord ($p<0.001$). The comparison of the mediolateral lengths between the SS cord and SS strap was not statistically significant ($p=0.096$). The infraspinatus, when compared to the whole supraspinatus, had a statistically larger humeral insertion area, anteroposterior width, and mediolateral length ($p<0.009$).

Table 5. All measurements for 3-D scanned tendons and humeral insertions.

Rotator Cuff Structure	Tendon Thickness [mm]	Tendon Area [mm²]	Humeral Insertion Area [mm²]	Humeral Insertion AP width [mm]	Humeral Insertion ML length [mm]
CHL	3.4 (2.1)	58.5 (39.3)	89.3 (29.6)	11.6 (2.2)	9.9 (1.9)
SS Cord	6.1 (1.7)	53.5 (23.7)	62.4 (20.1)	7.8 (1.3)	8.4 (1.6)
SS Strap	4.6 (2.3)	61.7 (28.4)	76.5 (19.1)	9.1 (1.6)	8.8 (1.4)
SS	5.3 (1.7)	115.2 (46.0)	138.9 (36.0)	16.9 (2.6)	8.6 (1.4)
IS	5.3 (2.0)	82.0 (36.1)	191.1 (75.5)	20.4 (3.9)	9.1 (1.4)

4.0 Discussion and Conclusions

The decrease in abduction force for a modeled SS cord tear with no compensating force from the SS strap (Cord: 0 N, Strap: 24 N) was found to be greater than that of a modeled SS strap tear with no added force (Cord: 56 N, Strap: 0 N). This is in line with the anatomical measurements for cross-sectional muscle area^{2,3,16}. If contribution to abduction force is directly parallel to the cross-sectional areas (140 mm² for the SS cord and 62 mm² for the SS strap), the SS cord would be capable of 2.3x the contractile force of the SS strap². The values found in this study do not reach the 2.3x threshold based on cross-sectional area alone, with the SS cord alone being responsible for 1.5x and 1.2x (at 0° and 30°, respectively) the abduction force of the SS strap alone. This suggests that the neighboring muscles and intersectional fibers assist in abduction when a tear is present^{16,17}. The force transmission may be routed through these surrounding structures and lessen the loss in strength.

Considering SS cord and SS strap tears with force compensation (Cord: 0 N, Strap: 80N and Cord: 80 N, Strap: 0 N), both tears resulted in a full return to native-state abduction force. There was no significant difference when comparing the two torn cases to the native case ($p \geq 0.291$) at both at 0° and 30° of humeral abduction. This ability to recover abduction strength despite a torn element of the SS is due to intratendinous connections between the anterior and posterior heads of the SS^{2,3,16}. A clinical implication from this finding is that small anterior or posterior rotator cuff tears can be treated conservatively, as the intact tendon will be able to account for the tear and produce normal abduction force¹⁸.

When examining the difference between a torn CHL and a torn SS cord, the greater decrease in abduction force was found to be with the SS cord-first group. Furthermore, the initial drop from

the CHL-first group was not statistically significant when compared to the native state ($p>0.999$), but the initial drop from the SS cord-first group was statistically significant ($p=0.030$). This signifies that the SS cord is the chief transmitter of abduction force among the SS cord and CHL. As the CHL can be viewed as the anterior insertion of the rotator cable, these findings would further suggest that the rotator cable does not stress-shield and that the SS cord is the more important structure in force transmission.

The findings in this study uphold the idea that the SS cord is thicker than the SS strap. The mediolateral thickness of the SS cord was found to be significantly larger than the SS strap, but there was no significant difference when comparing the cross-sectional areas of the SS cord and SS strap. In that the measurements were taken at half the distance between the tendon footprint and the musculotendinous junction, these thicknesses should not be taken as representative as the SS cord and SS strap units as a whole. However, this still raises a question about the assumption that the SS cord is more load bearing than the SS strap. The current findings, in parallel with our findings that the SS cord and SS strap both recover force when torn, suggest that the SS cord and SS strap may both be equally important in shoulder abduction strength.

The results from the three main focuses of this study can be combined for a clearer picture of the relationship between the CHL, SS cord, SS strap, and their roles in force transmission. The findings indicate that if the SS cord is damaged, the SS strap can and will take over the force transmission required and will produce abduction strength like an undamaged state. The same can be said for an intact SS cord compensating for a torn SS strap. This is important when taking the CHL into consideration as well, as the SS cord was shown to be more important in force transmission than the CHL. A torn CHL will not cause a reduction in abduction strength; it is shown that the SS cord will assist and result in normal abduction strength. An implication from

this study is that an intact SS strap may be able to compensate for a torn CHL, although further examinations would be needed to prove this. For clinicians, this suggests that small anterior or posterior rotator cuff tears (<10 mm width) can be treated conservatively, as the intact SS cord or SS strap will compensate for the torn portion and the patient's abduction strength will not suffer.

Appendix A MATLAB Code

Appendix A.1 Randomization MATLAB Code for Loading Case Sequences

```
%Austin Cook
%Loading Case Randomization
%7/1/22
%Generate the order of loading cases for shoulder abduction
%1 = Native
%2 = Load 1
%3 = Load 2
%4 = Load 3
%5 = Load 4
sequence = randperm(5,5);
disp(sequence)
```

Appendix A.2 Randomization MATLAB Code for Cutting Sequence

```
%Austin Cook
%Cutting Sequence Randomization
%7/1/22
%Generate random number determining whether the CHL or Cord is cut first
%1 = CHL
%2 = SS Cord
```

```
cutF = randperm(2,2);  
disp(cutF)
```

Bibliography

1. Reed, D., Cathers, I., Halaki, M., & Ginn, K. (2013). Does supraspinatus initiate shoulder abduction? *Journal of Electromyography and Kinesiology*, 23(2), 425–429. <https://doi.org/10.1016/j.jelekin.2012.11.008>).
2. Roh, M. S., Wang, V. M., April, E. W., Pollock, R. G., Bigliani, L. U., & Flatow, E. L. (2000). Anterior and posterior musculotendinous anatomy of the supraspinatus. *Journal of shoulder and elbow surgery*, 9(5), 436–440. <https://doi.org/10.1067/mse.2000.108387>.
3. Volk, A. G., & Vangsness, C. T., Jr (2001). An anatomic study of the supraspinatus muscle and tendon. *Clinical orthopaedics and related research*, (384), 280–285. <https://doi.org/10.1097/00003086-200103000-00032>.
4. Rothenberg A, Gasbarro G, Chlebeck J, Lin A. (2017). The Coracoacromial Ligament: Anatomy, Function, and Clinical Significance. *Orthop J Sports Med*. 2017 Apr 27;5(4):2325967117703398. doi: 10.1177/2325967117703398. PMID: 28508008; PMCID: PMC5415041.
5. Jeong, J. Y., Min, S. K., Park, K. M., Park, Y. B., Han, K. J., & Yoo, J. C. (2018). Location of Rotator Cuff Tear Initiation: A Magnetic Resonance Imaging Study of 191 Shoulders. *The American Journal of Sports Medicine*, 46(3), 649–655. <https://doi.org/10.1177/0363546517748925>).
6. Largacha, M., Parsons, I. M., Campbell, B., Titelman, R. M., Smith, K. L., & Matsen, F. (2006). Deficits in shoulder function and general health associated with sixteen common shoulder diagnoses: A study of 2674 patients. *Journal of Shoulder and Elbow Surgery*, 15(1), 30–39. <https://doi.org/10.1016/j.jse.2005.04.006>).
7. Kondo M., *Nihon Seikeigeka Gakkai Zasshi*. (1986). Study on the movement of the scapula during elevation of the arm. *Feb*;60(2):175-85. Japanese. PMID: 3722967.).
8. Ellenbecker TS Davies GJ. (2000). The application of isokinetics in testing and rehabilitation of the shoulder complex. *J Athl Train*. 2000;35:338-350.)
9. Lam JH, Bordonni B. Anatomy, Shoulder and Upper Limb, Arm Abductor Muscles. (2022). In: StatPearls [Internet]. Treasure Island (FL): StatPearls Publishing; 2022 Jan–. PMID: 30725833.).
10. DePalma A.F. (1950). Coracohumeral ligament. *Surgery of the shoulder*, J.B. Lippincott, Philadelphia (1950), pp. 23-24.
11. Ryuzo Arai, Akimoto Nimura, Kumiko Yamaguchi, Hideya Yoshimura, Hiroyuki Sugaya, Takahiko Saji, Shuichi Matsuda, Keiichi Akita. (2014). The anatomy of the coracohumeral

ligament and its relation to the subscapularis muscle, *Journal of Shoulder and Elbow Surgery*, Volume 23, Issue 10, 2014.

12. D.T. Harryman II, J. Sidles, S.L. Harris and F.A. Matsen III. (1992). The role of the rotator interval capsule in passive motion and stability of the shoulder. *J Bone Joint Surg Am*, 74 (1992), pp. 53-66.
13. Kedgley, A. E., Mackenzie, G. A., Ferreira, L. M., Drosdowech, D. S., King, G. J. W., Faber, K. J., & Johnson, J. A. (2007). The effect of muscle loading on the kinematics of in vitro glenohumeral abduction. *Journal of Biomechanics*, 40(13), 2953–2960. <https://doi.org/10.1016/j.jbiomech.2007.02.008>.
14. Omi, R., Sano, H., Ohnuma, M., Kishimoto, K. N., Watanuki, S., Tashiro, M., & Itoi, E. (2010). Function of the shoulder muscles during arm elevation: an assessment using positron emission tomography. *Journal of Anatomy*, 216(5), 643–649. <https://doi.org/10.1111/j.1469-7580.2010.01212.x>.
15. Rybalko D, Bobko A, Amirouche F, et al. (2020). Biomechanics in an Incomplete Versus Complete Supraspinatus Tear: A Cadaveric Study. *Orthopaedic Journal of Sports Medicine*. 2020;8(12). doi:10.1177/2325967120964476).
16. Clark, J. M., & Harryman, D. T., 2nd (1992). Tendons, ligaments, and capsule of the rotator cuff. *Gross and microscopic anatomy. The Journal of bone and joint surgery. American volume*, 74(5), 713–725.
17. Jost, B., Koch, P. P., & Gerber, C. (2000). Anatomy and functional aspects of the rotator interval. *Journal of shoulder and elbow surgery*, 9(4), 336–341. <https://doi.org/10.1067/mse.2000.106746>.
18. Kukkonen, J., Ryösä, A., Joukainen, A., Lehtinen, J., Kauko, T., Mattila, K., & Äärimaa, V. (2021). Operative versus conservative treatment of small, nontraumatic supraspinatus tears in patients older than 55 years: over 5-year follow-up of a randomized controlled trial. *Journal of shoulder and elbow surgery*, 30(11), 2455–2464. <https://doi.org/10.1016/j.jse.2021.03.133>.